Cathepsin S inhibitor reduces high-fat-induced adipogenesis, inflammatory infiltration, and hepatic lipid accumulation in obese mice

Jing Zheng[1], Huijun Zhuang[1], Tian Zhang[2], Yanni Wang[2], Ting Ran[2], Juan He[1], Na Han[1], Juan Duan[3]

[1]Department of Endocrinology, The Affiliated Hospital of Guizhou Medical University, Guiyang, China; [2]Guizhou Medical University, Guiyang, China; [3]Department of Traditional Chinese Medicine, Health Center of Hongqi Town, Zhuhai, China

Contributions: (I) Conception and design: J Zheng, H Zhuang; (II) Administrative support: T Zhang, Y Wang, T Ran; (III) Provision of study materials or patients: J Zheng, J He, J Duan; (IV) Collection and assembly of data: J Zheng, N Han; (V) Data analysis and interpretation: J Zheng, H Zhuang; (VI) Manuscript writing: All authors; (VII) Final approval of manuscript: All authors.

Correspondence to: Dr. Jing Zheng. Department of Endocrinology, The Affiliated Hospital of Guizhou Medical University, No. 28 Guiyi Street, Guiyang 550004, China. Email: Zhengjing_1122@163.com.

Background: Obesity, which results from a caloric intake and energy expenditure imbalance, is highly prevalent worldwide. Cathepsin S (CTSS), which is a cysteine protease, is elevated in obesity and may regulate a variety of physiological processes. This study sought to investigate the functional role of CTSS in obesity.

Methods: Mice were administrated 60 mg/kg of RO5444101 *in vivo* and fed a high-fat diet (HFD) to induce obesity. The weights of the mice fed a normal-chow diet and a HFD were measured. The expression levels of total triglycerides (TG), total cholesterol (TC), aspartate aminotransferase (AST), alanine aminotransferase (ALT), and monocyte chemoattractant protein-1 (MCP-1) were assessed using appropriate corresponding assay kits. Reverse transcription-quantitative polymerase chain reaction (RT-qPCR) was used to estimate the messenger ribonucleic acid (mRNA) expression of CTSS in the serum and the release of M1- and M2-type cytokines, and western blot was used to measure the phosphorylated-nuclear factor kappaB (NF-kappaB) p65 and NF-κB p65 proteins. The mRNA and protein expressions of sterol regulatory element-binding protein 1 (SREBP1), fatty acid synthase (FASN), leptin, and adiponectin were also evaluated by RT-qPCR and western blot. Further, hematoxylin and eosin (H&E), immunohistochemical, and red oil O staining were employed to detect the pathological changes of the epididymal white adipose tissue (eWAT), the macrophage infiltration in the eWAT, and lipid accumulation, respectively.

Results: We found that CTSS was elevated in the plasma, visceral adipose, and liver tissues of the obese mice. After the administration of 60 mg/kg of RO5444101, the weight of the obese mice decreased, insulin resistance was inhibited, and adipocyte formation was suppressed. The CTSS inhibitor also decreased the level of macrophage infiltration in the eWAT, MCP-1 expression, and the release of M1- and M2-type cytokines in the HFD-induced mice. The CTSS inhibitor appeared to improve the hepatic function parameters and lipid accumulation of the HFD-induced mice. The CTSS inhibitor also appeared to improve the inflammatory damage in the HFD-induced mice.

Conclusions: CTSS inhibitor helped to protect against HFD-induced adipogenesis, inflammatory infiltration, and hepatic lipid accumulation in obese mice.

Keywords: Obesity; cathepsin S inhibitor (CTSS inhibitor); adipogenesis; inflammatory infiltration; lipid accumulation

Submitted Sep 23, 2022. Accepted for publication Oct 31, 2022.

doi: 10.21037/atm-22-5145

View this article at: https://dx.doi.org/10.21037/atm-22-5145

Introduction

Obesity, which is defined as excessive body fat, has become a personal and public health problem worldwide (1). With approximately 46% of adults and 15% of children obese or overweight, China is the country most affected by obesity worldwide (2). Additionally, obesity has been reported to be closely related to the occurrence of numerous illnesses, including cardiovascular diseases and hypertension (3,4). Environmental factors, such as an unhealthy diet, insufficient physical exercise, fast food, ultra-processed foods, chemical contaminants, and the inflammatory response, are the main causes of obesity (5,6). Interventions directed at environmental factors and inflammation have been shown to effectively address obesity; however, the efficacy of such interventions has been limited (7,8). Thus, other intervention methods need to be developed to treat obesity.

Cathepsin S (CTSS), which is a critical member of the cysteine proteinase family, is a strong mammalian elastase and can degrade a variety of extracellular components, including elastin, fibronectin, laminin, and collagen (9,10). An increasing number of studies have shown that CTSS is closely associated with the advancement of many diseases; for example, in atherosclerosis, the messenger ribonucleic acid (mRNA) expression of CTSS was found to be greatly elevated in infract areas (11). Chang and coworkers have evidenced that CTSS promoted the development of pulmonary arterial hypertension (12). Further, CTSS has been shown to be abundant in many tumor cells and to participate in the progression of cancers (13). Notably, previous studies have reported that CTSS, which is elevated in obese individuals, contributed to the expansion of fat mass in obesity due to its facilitative effects on adipogenesis (14,15). Interestingly, Ahmad *et al.* have evidenced that CTSS inhibitor might be a potential therapeutic target for obese patients (16).

To induce obesity *in vivo*, the mice in this study were fed a high-fat diet (HFD). This study was designed to examine the functions of CTSS in adipogenesis, inflammatory infiltration, and hepatic lipid accumulation in obese mice. Our findings may lay a foundation for further research on obesity in the future. We present the following article in accordance with the ARRIVE reporting checklist (available at https://atm.amegroups.com/article/view/10.21037/atm-22-5145/rc).

Methods

Mice and diet

Male C57BL/6J (7-week-old) mice were provided by Vital River Laboratory Animals Technology Co., Ltd., (Beijing, China). The mice were housed in temperature-controlled cages and placed on a 12-h light/dark cycle with free access to food and water. Following 7 days of adaption, the 24 mice were randomly divided into the following 3 groups: (I) the Control group; (II) the HFD group; and (III) the HFD + CTSS inhibitor group (n=8 per group). The mice in the Control group were fed a normal-chow (NC) diet containing 10% of calories from fat (17). The mice in the HFD group were fed a HFD with 60% of calories from fat (17). The mice in the HFD + CTSS inhibitor group were fed the same diet as that as mice in the HFD group but also received 60 mg/kg of RO5444101 (18).

After 12 weeks of feeding, the mice were euthanized, and fat depots from epididymal white adipose tissue (eWAT), plasma samples, and liver tissues were rapidly removed, immediately frozen in liquid nitrogen, and stored at –80 ℃ awaiting the follow-up experiments. No signs of peritonitis, pain, or discomfort were observed after the mice had been euthanized. A protocol was prepared before the study without registration. Animal experiments were performed under a project license (No. 2200596) granted by the ethics board of Guizhou Medical University in compliance with Guizhou Medical University guidelines for the care and use of animals.

Biochemical analyses

Whole blood was centrifuged at 3,000 g for 10 min at 4 ℃ to collect the serum for measurements of alanine aminotransferase (ALT) and aspartate aminotransferase (AST), triglyceride (TG) and total cholesterol (TC) as previously described (19,20).

Measurement of hepatic TG

For the purpose of detecting hepatic TG, the homogenization of liver tissue with 300 μg/mL PBS (pH 7.4) and stainless-steel beads (Qiagen, Hilden, Germany) was implemented at 30 frequency/s for 1 min by virtue of a homogenizer (TissueLyser II; Qiagen) in light of standard

protocol. After the centrifugation of homogenates, TG quantification kit (Cell Biolabs, San Diego, CA, USA) was applied for the assessment of hepatic TG in the supernatant.

Reverse transcription-quantitative polymerase chain reaction (RT-qPCR)

The total ribonucleic acid (RNA) was extracted from the sample tissues using Trizol® reagent (Guangzhou Saiyan Biotechnology Co., Ltd., Guangzhou, China) and then transcribed into complementary deoxyribonucleic acid (cDNA) using a commercial RevertAid™ cDNA synthesis kit (Beijing Zhijie Fangyuan Technology Co., Ltd., Beijing, China). Using an iTaq Universal SYBR Green kit (Bio-Rad Laboratories, Inc., Hercules, CA, USA), RT-qPCR was performed in accordance with the standard protocol. The required thermocycling conditions were set as follows: Initial denaturation at 95 ℃ for 8 min; denaturation at 95 ℃ for 25 sec; annealing at 60 ℃ for 30 sec; extension at 72 ℃ for 30 sec; and a final extension at 72 ℃ for 10 min. Finally, $2^{-\Delta\Delta Ct}$ method was adopted to calculate the relative gene expression (21) and glyceraldehyde3-phosphate dehydrogenase (GAPDH) acted as the endogenous control. The following primer sequences were used: CTSS forward primer: 5'-CCATTGGGATCTCTGGAAGAAAA-3', reverse primer: 5'-TCATGCCCACTTGGTAGGTAT-3'; sterol regulatory element-binding protein 1 (SREBP1) forward primer: 5'-TGGGAACCCTGTTTGTGTCC-3', reverse primer: 5'-TGTGGATGCCGACCAGATTC-3'; fatty acid synthase (FASN) forward primer: 5'-GGAGGTGGTGATAGCCGGTAT-3', reverse primer: 5'-TGGGTAATCCATAGAGCCCAG-3'; leptin forward primer: 5'-ATGTGCCCTTCCGATATACAACC-3', reverse primer: 5'-CGTGTCATCCACTAATCTTCTGG-3'; adiponectin forward primer: 5'-GCCAAACACCGATTGGGGT-3', reverse primer: 5'-GGCTCCAAATCTCCTTGGTAGTT-3'; inducible nitric oxide synthase (iNOS) forward primer: 5'-CTCTTCGACGACCCAGAAAAC-3', reverse primer: 5'-CAAGGCCATGAAGTGAGGCTT-3'; tumor necrosis factor-alpha (TNF-α) forward primer: 5'-AAACCACCAAGTGGAGGAGC-3', reverse primer: 5'-GCAGCCTTGTCCCTTGAAGA-3'; interleukin (IL)-1β forward primer: 5'- GTCGCTCAGGGTCACAAGAA-3', reverse primer: 5'-CAAAGCAATGTGCTGGTGCT-3'; IL-6 forward primer: 5'-GGCGGATCGGATGTTGTGAT-3', reverse primer: 5'-GGACCCCAGACAATCGGTTG-3'; arginase 1 (Arg1) forward primer: 5'-CTCCAAGCCAAAGTCCTTAGAG-3', reverse primer: 5'-GGAGCTGTCATTAGGGACATCA-3'; IL-10 forward primer: 5'-TGAGGCGCTGTCATCGATTT-3', reverse primer: 5'-TGCTTCCCAAGGAAGAACCC-3' or GAPDH forward primer: 5'-AATGGATTTGGACGCATTGGT-3', reverse primer: 5'-TTTGCACTGGTACGTGTTGAT-3'.

Western blot

The total proteins were extracted from the sample using radioimmunoprecipitation assay lysis buffer (Shanghai Absin Biotechnology Co., Ltd., Shanghai, China) and were quantified using a bicinchoninic acid protein assay kit (Shanghai Yisheng Biotechnology Co., Ltd., Shanghai, China). After the exposure to 8% sodium dodecyl sulfate-polyacrylamide gel electrophoresis, the transferring of proteins to polyvinylidene fluoride membranes was performed. The membranes that blocked with 5% non-fat milk were incubated overnight at 4 ℃ with primary antibodies targeting CTSS (ab232740; 1:1,000; Abcam), SREPB1 (ab28481; 1:1,000; Abcam), FASN (ab128870; 1:1,0000; Abcam), leptin (ab16227; 1:1,000; Abcam), adiponectin (ab181281; 1:1,000; Abcam), phosphorylated-nuclear factor kappaB (NF-κB) p65 (ab76302; 1:1,000; Abcam), NF-κB p65 (ab32536; 1:1,000; Abcam), or GAPDH (ab9485; 1:2,500; Abcam). Next, the membranes got cultivated with a horseradish peroxidase–linked anti-mouse secondary antibody (ab6728; 1:2,000; Abcam) at room temperature for 2 h. Finally, the visualization of protein bands was implemented by enhanced chemiluminescence (Yeasen Biotech) and Image J (Version 146) was employed for analysis.

Glucose tolerance test (GTT) and insulin tolerance test (ITT)

Following the feeding for 12 weeks, the mice were subjected to a GTT and an ITT following an overnight fast. After collecting the baseline blood, the intraperitoneal injection of mice with glucose (0.9 g/kg body weight) and insulin (0.75 units/kg body weight) was carried out. In the tail vein blood samples, the appraisement of blood glucose levels was implemented 15, 30, 60, 90 and 120 min after the injection by means of a blood glucometer (One Touch, Milpitas, CA, USA).

Histological examination and immunohistochemistry

The collected eWAT was subjected to 4% paraformaldehyde

fixation. Following the dehydration and embedment in paraffin, the cutting of sample sections was operated by means of a Leica RM22559 microtome (Leica, Shanghai, China), stained with standard hematoxylin and eosin (H&E) staining in light of standard protocol and got analyzed via immunohistochemical staining of F4/80 (Bio-Rad, Hercules, CA, USA) as described previously (19,20).

Oil red O staining

Following the collection of the liver tissue, oil red O staining was applied to observe lipid accumulation. The tissue was pre-rinsed with phosphate buffered solution (PBS) and then fixed with 4% paraformaldehyde for 30 min. The tissue was then rinsed with PBS again, after which the tissue was stained with 1% filtered red oil O solution for 30 min. The positive oil red O areas (the stained areas) were observed using an inverted microscope, and the total lipid content was determined.

Statistical analysis

All the collected data that presented in the form of the mean ± standard deviation (SD) got analyzed with the help of GraphPad Prism 8.0 software (GraphPad software, Inc., CA, USA). The Student's *t*-test was adopted to compare differences between 2 groups, and a 1-way analysis of variance (ANOVA) with Tukey's post-hoc test was used to compare differences among multiple groups. A P value <0.05 was considered statistically significant.

Results

CTSS expression was increased in the plasma, visceral adipose, and liver tissue of the obese mice

After feeding for 12 weeks, the mice were sacrificed, and their weight was measured. Relative to the Control group, the weight of the mice in the HFD group was conspicuously increased (*Figure 1A*). The results obtained from the TG and TC assay kits revealed that the mice fed a HFD had higher expressions of TC and TG compared to those fed a NC diet (*Figure 1B,1C*). Additionally, the mRNA expression of CTSS in the plasma of the mice was assessed by RT-qPCR, and the results showed that the mRNA expression of CTSS of the mice in the HFD group was significantly elevated compared to that of mice in the Control group (*Figure 1D*). Further, the mRNA and protein expression levels of CTSS in the visceral adipose tissue of the mice in the HFD group were significantly increased compared to those of mice in the Control group (*Figure 1E,1F*). Moreover, the expression of CTSS at both the mRNA and protein levels in the liver tissue of the obese mice was also increased (*Figure 1G,1H*).

The CTSS inhibitor reduced body weight and insulin resistance in the obese mice

The weight of the mice was measured every 2 weeks, and the results indicated that the weight of the mice in the HFD group was significantly increased compared to that of the mice in the Control group. The CTSS inhibitor produced an opposite effect on the weight of the mice, as evidenced by the decreased weight of the mice in the HFD + CTSS inhibitor group compared to that of the HDF group (*Figure 2A*). As *Figure 2B,2C* show, the elevated glucose tolerance and insulin tolerance of the mice in the HFD group was reduced after the administration of the CTSS inhibitor. Thus, the CTSS inhibitor had a suppressive effect on the body weight and insulin resistance of the obese mice.

The CTSS inhibitor reduced adipocyte formation in obese mice

The H&E staining revealed that the pathological changes in the eWAT of the obese mice improved after treatment with the CTSS inhibitor (*Figure 3A*). Relative to the Control group, the diameter of the adipocytes was greatly elevated in the mice in the HFD group, which was then offset by the CTSS inhibitor treatment (*Figure 3B*). Additionally, the expressions of SREBP1, FASN, and leptin were significantly increased while the expression of adiponectin was decreased in the obese mice compared to the mice in the Control group; however, the administration of the CTSS inhibitor reversed the effects of the HFD on the mice as shown by the decreased levels of SREBP1, FASN, leptin and adiponectin in the mice in the HFD + CTSS inhibitor group (*Figure 3C,3D*).

The CTSS inhibitor reduced adipose tissue macrophage infiltration in the obese mice

The elevated F4/80 level of the mice fed a HFD was reduced by the administration of the CTSS inhibitor (*Figure 4A*). Similarly, CTSS treatment also reduced the expression of monocyte chemoattractant protein-1 (MCP-1) in the

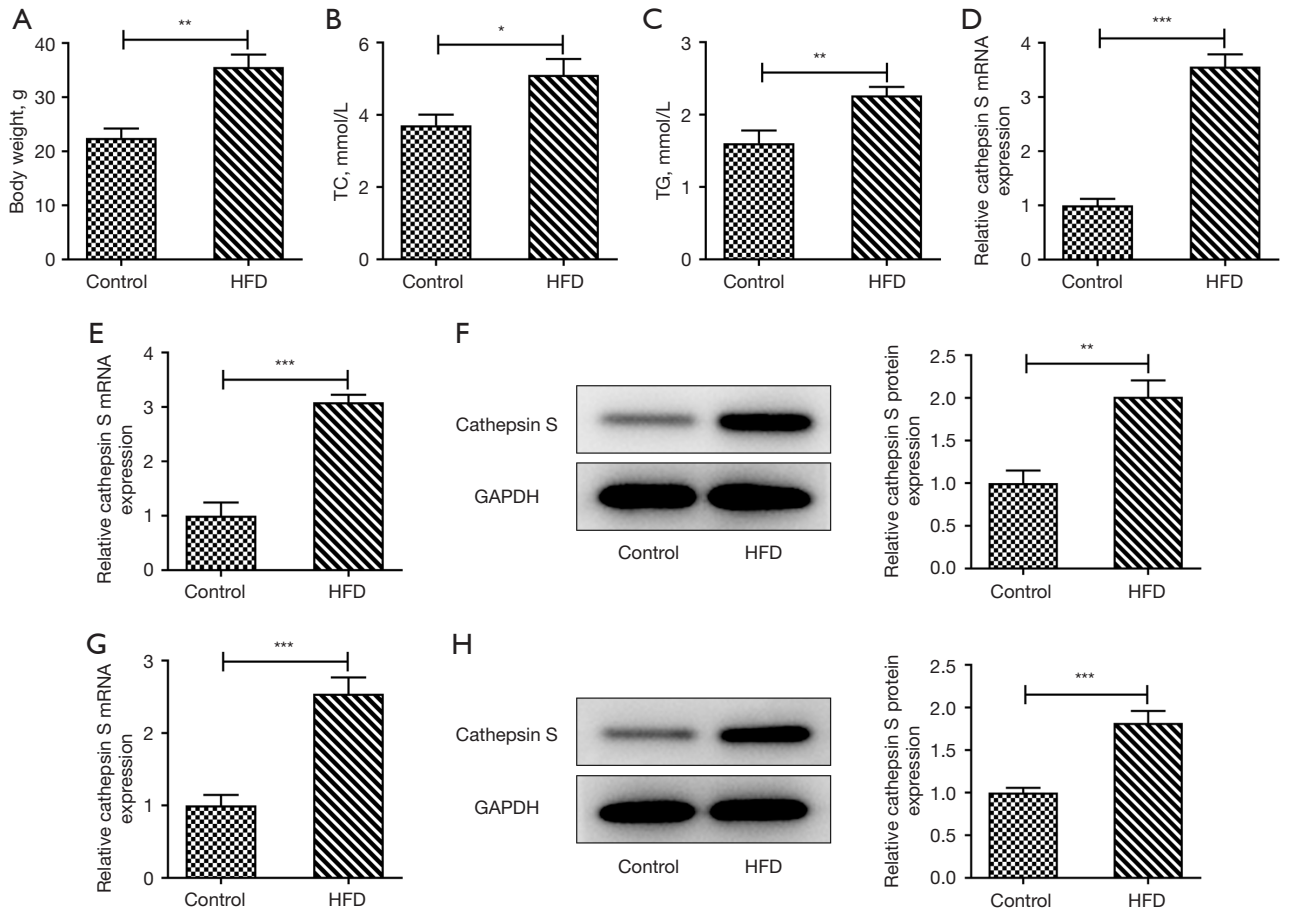

Figure 1 CTSS expression was increased in the plasma, visceral adipose, and liver tissue of the obese mice. (A) The body weight of the mice. (B) The level of TC. (C) The level of TG. (D) The mRNA expression of CTSS in the plasma of the mice was detected by RT-qPCR. (E,F) The mRNA and protein expressions of CTSS in the visceral adipose tissue of the mice were detected by RT-qPCR and western blot. (G,H) The mRNA and protein expressions of CTSS in the liver tissue of the mice were detected by RT-qPCR and western blot. *, P<0.05; **, P<0.01; ***, P<0.001. HFD, high-fat diet; TC, total cholesterol; TG, total triglycerides; mRNA, messenger ribonucleic acid; GAPDH, glyceraldehyde-3-phosphate dehydrogenase; CTSS, cathepsin S; RT-qPCR, reverse transcription-quantitative polymerase chain reaction.

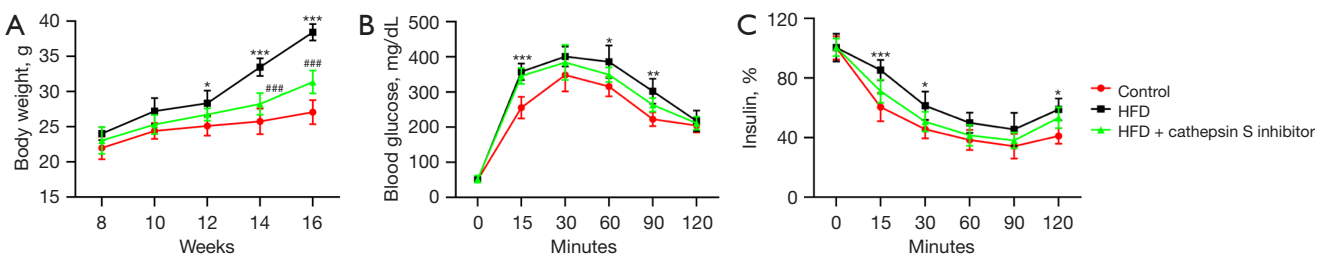

Figure 2 The CTSS inhibitor reduced the body weight and insulin resistance of the obese mice. (A) Changes in the weight of the mice. (B) The GTT. (C) The ITT. *, P<0.05; **, P<0.01; ***, P<0.001, ###, P<0.001. HFD, high-fat diet; CTSS, cathepsin S; GTT, glucose tolerance test; ITT, insulin tolerance test.

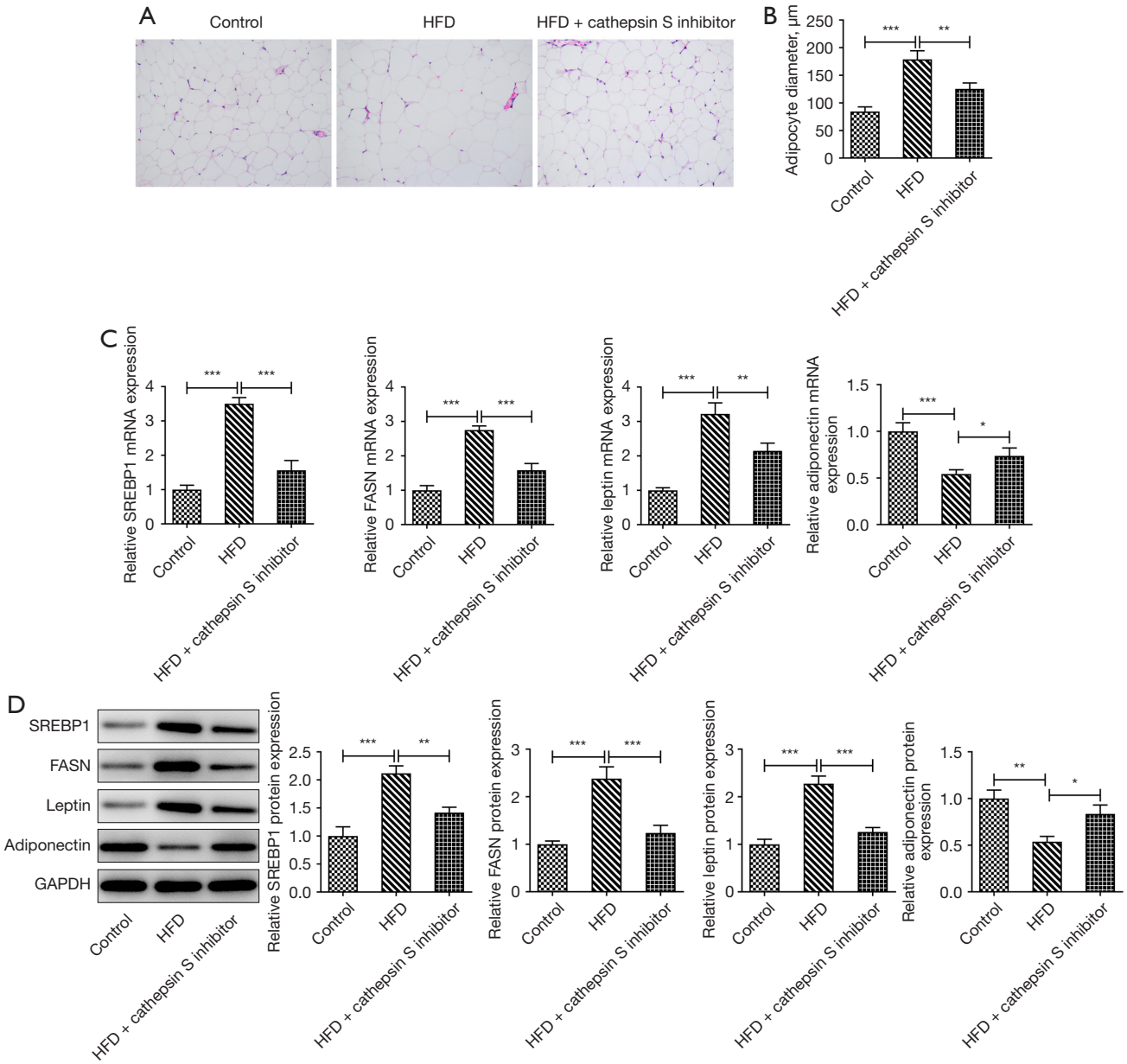

Figure 3 The CTSS inhibitor reduced adipocyte formation in obese mice. (A) The staining of eWAT with H&E. (Magnification, ×200). (B) The diameter of the adipocyte. (C,D) The mRNA and protein expressions of SREBP1, FASN, leptin, and adiponectin were detected by RT-qPCR and western blot. *, P<0.05; **, P<0.01; ***, P<0.001. HFD, high-fat diet; mRNA, messenger ribonucleic acid; GAPDH, glyceraldehyde-3-phosphate dehydrogenase; CTSS, cathepsin S; eWAT, epididymal white adipose tissue; H&E, hematoxylin and eosin; RT-qPCR, reverse transcription-quantitative polymerase chain reaction.

obese mice (*Figure 4B*). Additionally, a HFD significantly increased the contents of iNOS, TNF-α, IL-1β, and IL-6 in the obese mice relative with those of the mice in the Control group, but the administration of the CTSS inhibitor decreased these levels (*Figure 4C-4F*). Notably, the administration of the CTSS inhibitor further enhanced the decrease in the Arg1 and IL-10 levels of the HFD mice (*Figure 4G,4H*). Moreover, the CTSS inhibitor reduced the increased protein content of p-NF-κB p65 in the obese mice (*Figure 4I*). Collectively, these results implied that

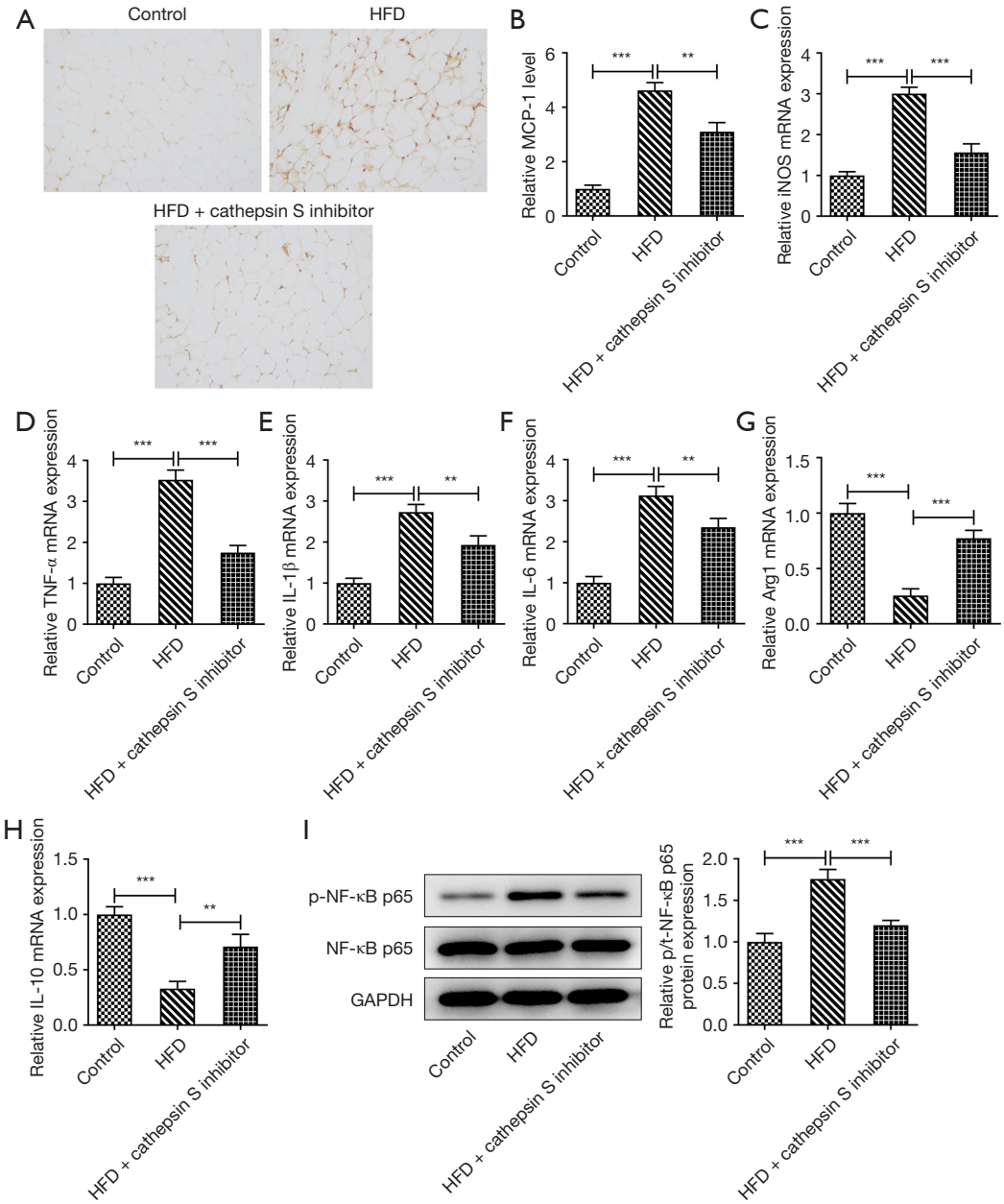

Figure 4 The CTSS inhibitor reduced adipose tissue macrophage infiltration in the obese mice. (A) The levels of macrophage infiltration in the eWAT adipose tissue were detected by the immunohistochemical staining of F4/80. (Magnification, ×200). (B) The expression of MCP-1 was detected using the corresponding assay kit. (C-F) The mRNA expressions of iNOS, TNF-α, IL-1β, and IL-6 in M1 were detected by RT-qPCR. (G,H) The mRNA expressions of Arg1 and IL-10 in M2 were detected by RT-qPCR. (I) The protein expressions of p-NF-κB p65 and NF-κB p65 were detected by western blot. **, P<0.01; ***, P<0.001. HFD, high-fat diet; MCP-1, monocyte chemoattractant protein-1; iNOS, inducible nitric oxide synthase; mRNA, messenger ribonucleic acid; TNF-α, tumor necrosis factor-alpha; IL, interleukin; NF-κB, nuclear factor kappaB; GAPDH, glyceraldehyde-3-phosphate dehydrogenase; CTSS, cathepsin S; eWAT, epididymal white adipose tissue; RT-qPCR, reverse transcription-quantitative polymerase chain reaction.

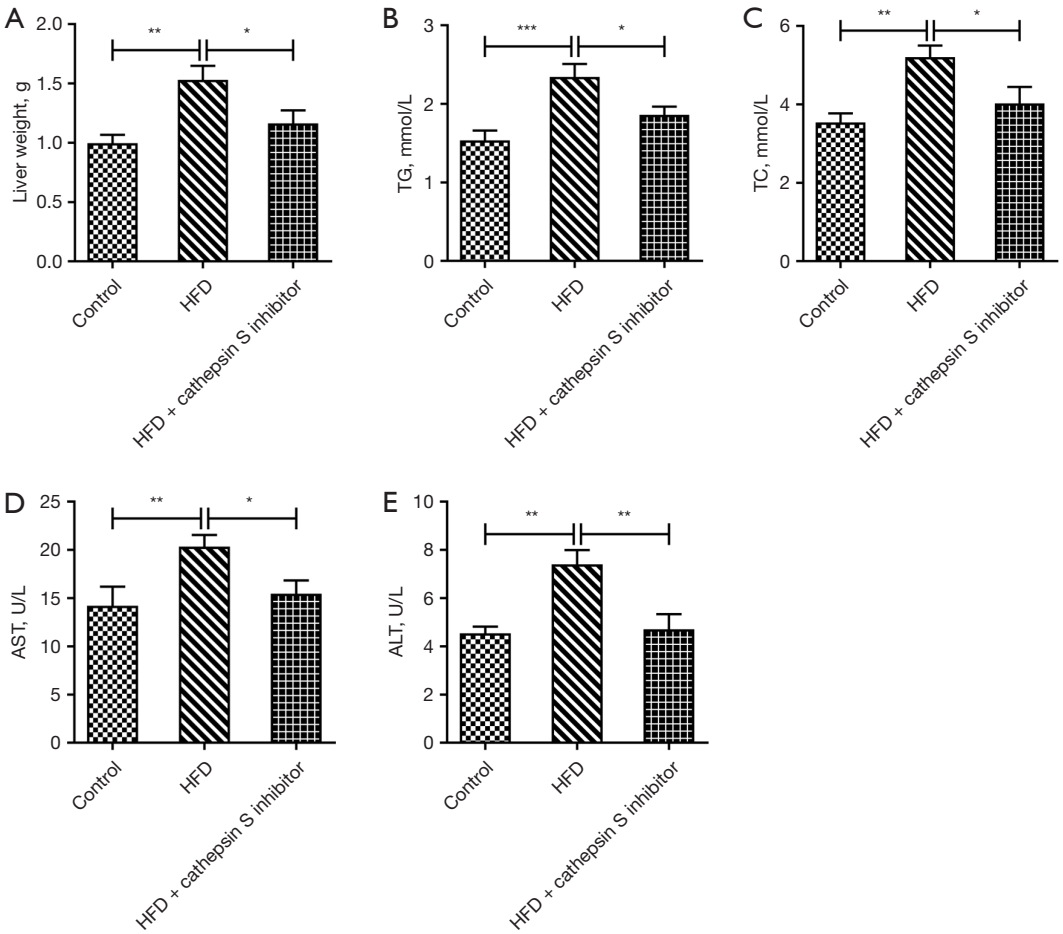

Figure 5 The CTSS inhibitor improved the hepatic function parameters in the obese mice. (A) The liver weight of the mice. (B) The level of TG. (C) The level of TC. (D) The expression of AST in the plasma. (E) The expression of ALT in the plasma. *, P<0.05; **, P<0.01; ***, P<0.001. HFD, high-fat diet; TG, total triglycerides; TC, total cholesterol; AST, aspartate aminotransferase; ALT, alanine aminotransferase; CTSS, cathepsin S.

the CTSS inhibitor reduced adipose tissue macrophage infiltration in the obese mice.

The CTSS inhibitor improved the hepatic function parameters in obese mice

The liver weights of the mice were measured, and the results showed that the mice in the HFD group had an increased liver weight compared to that of the Control group, but this effect was subsequently reversed by the administration of the CTSS inhibitor (*Figure 5A*). Additionally, the CTSS inhibitor also had suppressive effects on TG and TC in the obese mice, as demonstrated by decreased levels of TG and TC in the HFD + CTSS inhibitor group relative to the HFD group (*Figure 5B,5C*). As *Figure 5D,5E* show, the elevated levels of AST and ALT in the serum of the mice fed a HFD were decreased following the administration of the CTSS inhibitor. The above results revealed that the CTSS inhibitor helped to improve the hepatic function parameters of the obese mice.

The CTSS inhibitor improved hepatic lipid accumulation in the obese mice

The oil red O staining results showed that a larger number of red lipid particles were observed in the HFD group compared to the Control group, which were then diminished by the CTSS inhibitor. Thus, the CTSS

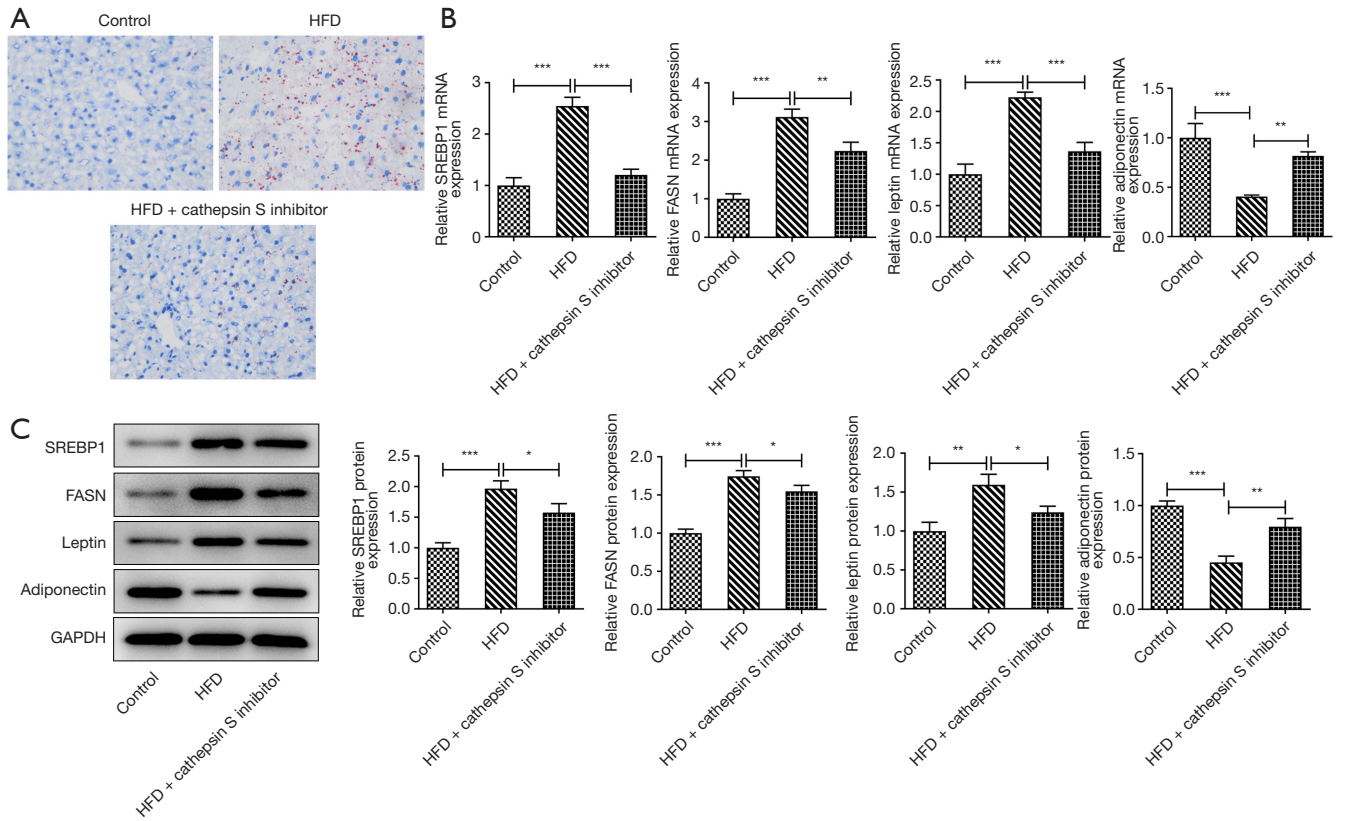

Figure 6 The CTSS inhibitor improved hepatic lipid accumulation in the obese mice. (A) Lipid accumulation was detected by oil red O staining. (Magnification, ×400). (B,C) The mRNA and protein expressions of SREBP1, FASN, leptin, and adiponectin were detected by RT-qPCR and western blot. *, P<0.05; **, P<0.01; ***, P<0.001. HFD, high-fat diet; mRNA, messenger ribonucleic acid; GAPDH, glyceraldehyde-3-phosphate dehydrogenase; CTSS, cathepsin S; RT-qPCR, reverse transcription-quantitative polymerase chain reaction.

inhibitor had a suppressive effect on the lipid accumulation of the obese mice (*Figure 6A*). Additionally, a HFD significantly increased the expression of SREBP1, FASN, and leptin but decreased the expression of adiponectin in the mice in the HFD group compared to the Control group, but these effects were then reversed by the administration of the CTSS inhibitor (*Figure 6B,6C*). To sum up, the CTSS inhibitor helped to improve hepatic lipid accumulation in the obese mice.

The CTSS inhibitor improved the inflammatory cytokines release of hepatic tissue in the obese mice

As *Figure 7A-7F* showed, a HFD enhanced the mRNA contents of iNOS, TNF-α, IL-1β, and IL-6 but decreased the mRNA contents of Arg1 and IL-10 in the HFD mice group compared to the Control group, while the CTSS inhibitor produced the opposite effects on these factors, as evidenced by decreased contents of iNOS, TNF-α, IL-1β and IL-6 and increased contents of Arg1 and IL-10 in the HFD + CTSS inhibitor group. Further, the enhanced protein expression of p-NF-κB p65 in the HFD-induced mice was reduced by the administration of the CTSS inhibitor (*Figure 7G*). Thus, the CTSS inhibitor helped to improve the inflammatory cytokines release of hepatic tissue in the obese mice.

Discussion

Obesity, which has become more prevalent in recent years, has a close association with metabolic disturbances, including insulin resistance and inflammation (22,23). CTSS, which is a member of the cysteine cathepsin proteases family, is involved in a variety of cellular processes (24,25). Further, numerous studies have shown that CTSS is involved in many diseases; for example, CTSS expression was shown to be

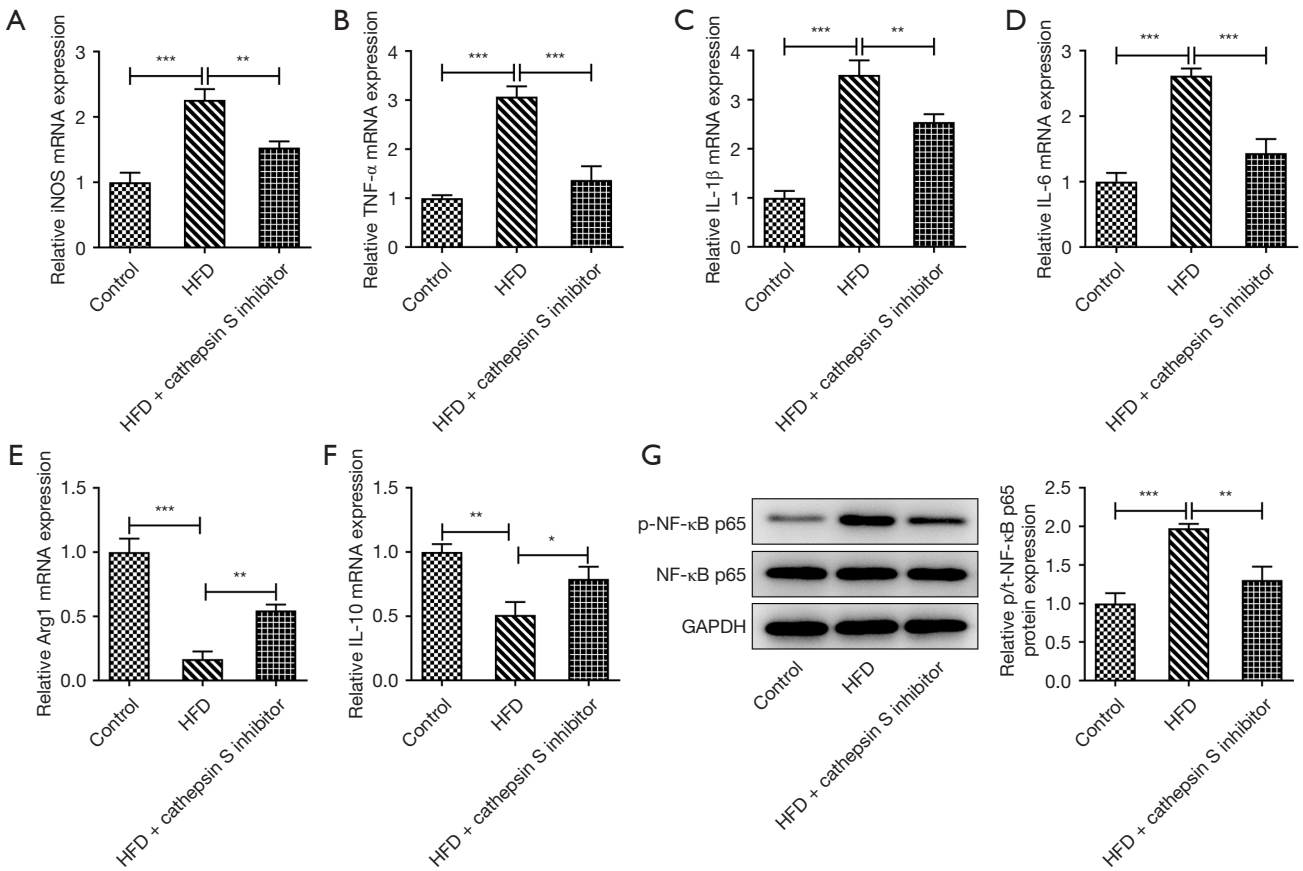

Figure 7 The CTSS inhibitor improved the inflammatory cytokines release of hepatic tissue in the obese mice. (A-D) The mRNA expressions of iNOS, TNF-α, IL-1β, and IL-6 in M1 were detected by RT-qPCR. (E,F) The mRNA expressions of Arg1 and IL-10 in M2 were detected by RT-qPCR. (G) The protein expressions of p-NF-κB p65 and NF-κB p65 were detected by western blot. *, P<0.05; **, P<0.01; ***, P<0.001. iNOS, inducible nitric oxide synthase; mRNA, messenger ribonucleic acid; HFD, high-fat diet; TNF-α, tumor necrosis factor-alpha; IL, interleukin; NF-κB, nuclear factor kappaB; GAPDH, glyceraldehyde-3-phosphate dehydrogenase; CTSS, cathepsin S; RT-qPCR, reverse transcription-quantitative polymerase chain reaction.

greatly elevated in hydronephrotic kidneys (26). Similarly, Kawato *et al.* found that CTSS expression was abundant in the plasma of patients or mice suffering from systemic lupus erythematosus (27). Evidently, CTSS is abnormally expressed in many diseases, including obesity. A previous study showed that CTSS expression is elevated in obese mice (28).

In the present study, a mice model of obesity was established by feeding the mice a HFD. After 12 weeks of feeding, the weight of the mice fed a HFD mice had significantly increased. Additionally, CTSS expression was discovered to be significantly increased in the plasma, visceral adipose, and liver tissue of the HFD-induced mice, which supports the results of Rauner *et al.* (28). After the administration of RO5444101, which is a selective inhibitor of CTSS, the weight of the obese mice decreased significantly.

An increasing number of studies have demonstrated that CTSS inhibitor has the potential to be a therapeutic target for many diseases. For example, CTSS inhibitor was reported to be effective for the therapy of pulmonary fibrosis (29). Additionally, Wei and co-workerd have evidenced that the CTSS inhibitor-Z-FL-COCHO (ZFL) could attenuate TGF-β-induced invasive growth in glioblastoma cells (30). Interestingly, the inhibition of CTSS activity could reduce lipid content and expression of adipocyte markers in obesity (14). Obesity leads to the excessive accumulation of WAT, which primarily consists of adipocytes that store lipid, and acts as a critical player in

controlling the energy homeostasis of the whole body (31). It is well-documented that the prevention of adipogenesis might be a promising therapeutic method for obesity (32). In the present study, we discovered that the pathological changes of eWAT in the obese mice were improved by administering the CTSS inhibitor. Additionally, the diameter of adipocytes also decreased following the administration of the CTSS inhibitor. SREBP1 and adiponectin are important genes in repressing adipogenesis (33,34). In this study, the elevated mRNA and protein expressions of SREBP1, FASN, and leptin and the reduced expression of adiponectin in the obese mice were reversed by the CTSS inhibitor. Thus, the CTSS inhibitor had suppressive effects on the adipocyte formation in obese mice. Moreover, the expansion of WAT could contribute to the dysfunction of insulin resistance and glucose tolerance (35,36). The enhanced glucose tolerance and insulin resistance of the obese mice that resulted from being fed a HFD were diminished after the administration of the CTSS inhibitor.

The expansion of adipose tissue in obesity is characterized by increased infiltration of pro-inflammatory immune cells into adipose tissue, resulting in chronic and low-grade inflammation (37). Inflammatory infiltration interventions might provide an underlying therapeutic approach for treating obesity. In this study, we observed that the increased level of macrophage infiltration in eWAT adipose tissue of the obese mice was suppressed by the CTSS inhibitor.

The expanded adipocyte-derived free fatty acid and the chemotactic factor MCP-1 have been reported to have promotive effects on the trigger of pro-inflammatory M1- rather than anti-inflammatory M2-macrophage subsets in obese adipose tissue (38,39). In the present study, the CTSS inhibitor decreased the expression of MCP-1 in the eWAT adipose tissue of the obese mice. Further, research has shown that the M1-dominant macrophage phenotype results in the excessive release of pro-inflammatory factors (40). In the present study, we found that a HFD increased levels of iNOS, TNF-α, IL-1β, and IL-6 in mice, which were then decreased by the CTSS inhibitor. Arg1 is a marker of M2 (41). The decreased levels of Arg1 and IL-10 in the mice resulting from HFD induction were increased by the CTSS inhibitor. Other research has shown that the excessive generation of pro-inflammatory factors is closely related to the triggering of NF-κB inflammatory signaling (17).

For adipose tissue, the liver, which is a vital metabolic organ, serves as a critical player in lipid distribution and energy metabolism (42). It was reported that the prevention of hepatic lipid accumulation in obese mice can be achieved through many ways. For instance, policosanol attenuated hepatic lipid accumulation in mice by regulating AMPK-FXR-TGR5 cross-talk (43). In addition, Han et al have testified that the depletion of gut microbiota could suppress hepatic lipid accumulation in HFD-fed mice (44). In this study, we initially investigated the hepatic function parameters of the obese mice before exploring the lipid accumulation. We found that the elevated levels of TG, TC, AST and ALT in the HFD-induced obese mice were decreased after the administration of the CTSS inhibitor. Thus, CTSS inhibition appears to improve hepatic function parameters in obesity. Lee *et al.* reported that the suppression of lipid accumulation helps to protect against adipogenesis and HFD-induced obesity (45). Notably, the increased number of red lipid particles in the mice fed a HFD was later diminished by the CTSS inhibitor, which was also accompanied by decreases in the expression of SREBP1, FASN, and leptin and an increase in the expression of adiponectin.

Conclusions

To sum up, this study revealed the effects of CTSS inhibition on adipogenesis, inflammatory infiltration, and hepatic lipid accumulation in HFD-induced obese mice. Our findings provide a solid foundation for the exploration of therapeutic methods for obesity. However, this study also had some limitations. For example, the effects of CTSS inhibition on human obesity in a clinical setting were not explored.

Acknowledgments

Funding: The present study was supported by the National Natural Science Foundation of China (Grant Nos. 82260175, 81860161), National Natural Science Foundation of Guizhou Medical University (No. 19NSP052) and Doctoral Starting Fund Project of Guizhou Medical University (No. (2020) 076).

Footnote

Reporting Checklist: The authors have completed the ARRIVE reporting checklist. Available at https://atm.amegroups.com/article/view/10.21037/atm-22-5145/rc

Data Sharing Statement: Available at https://atm.amegroups.

com/article/view/10.21037/atm-22-5145/dss

Conflicts of Interest: All authors have completed the ICMJE uniform disclosure form (available at https://atm.amegroups.com/article/view/10.21037/atm-22-5145/coif). The authors have no conflicts of interest to declare.

Ethical Statement: The authors are accountable for all aspects of the work in ensuring that questions related to the accuracy or integrity of any part of the work are appropriately investigated and resolved. Animal experiments were performed under a project license (No. 2200596) granted by the ethics board of Guizhou Medical University in compliance with Guizhou Medical University guidelines for the care and use of animals.

References

1. Damanaki A, Memmert S, Nokhbehsaim M, et al. Effects of Obesity on Bone Healing in Rats. Int J Mol Sci 2021;22:13339.
2. Wang Y, Xue H, Sun M, et al. Prevention and control of obesity in China. Lancet Glob Health 2019;7:e1166-7.
3. Ren J, Wu NN, Wang S, et al. Obesity cardiomyopathy: evidence, mechanisms, and therapeutic implications. Physiol Rev 2021;101:1745-807.
4. Zhao W, Mo L, Pang Y. Hypertension in adolescents: The role of obesity and family history. J Clin Hypertens (Greenwich) 2021;23:2065-70.
5. Mayoral LP, Andrade GM, Mayoral EP, et al. Obesity subtypes, related biomarkers & heterogeneity. Indian J Med Res 2020;151:11-21.
6. Monteiro R, Azevedo I. Chronic inflammation in obesity and the metabolic syndrome. Mediators Inflamm 2010;2010:289645.
7. Kuder MM, Nyenhuis SM. Optimizing lifestyle interventions in adult patients with comorbid asthma and obesity. Ther Adv Respir Dis 2020;14:1753466620906323.
8. Sharma V, Cowan DC. Obesity, Inflammation, and Severe Asthma: an Update. Curr Allergy Asthma Rep 2021;21:46.
9. Cheng XW, Shi GP, Kuzuya M, et al. Role for cysteine protease cathepsins in heart disease: focus on biology and mechanisms with clinical implication. Circulation 2012;125:1551-62.
10. Jing Y, Shi J, Lu B, et al. Association of Circulating Cathepsin S and Cardiovascular Disease Among Patients With Type 2 Diabetes: A Cross-Sectional Community-Based Study. Front Endocrinol (Lausanne) 2021;12:615913.
11. Chen H, Wang J, Xiang MX, et al. Cathepsin S-mediated fibroblast trans-differentiation contributes to left ventricular remodelling after myocardial infarction. Cardiovasc Res 2013;100:84-94.
12. Chang CJ, Hsu HC, Ho WJ, et al. Cathepsin S promotes the development of pulmonary arterial hypertension. Am J Physiol Lung Cell Mol Physiol 2019;317:L1-L13.
13. Ghanadi K, Ashorzadeh S, Aliyepoor A, et al. Evaluation of serum levels of cathepsin S among colorectal cancer patients. Ann Med Surg (Lond) 2022;78:103831.
14. Taleb S, Cancello R, Clément K, et al. Cathepsin s promotes human preadipocyte differentiation: possible involvement of fibronectin degradation. Endocrinology 2006;147:4950-9.
15. Karimkhanloo H, Keenan SN, Sun EW, et al. Circulating cathepsin S improves glycaemic control in mice. J Endocrinol 2021;248:167-79.
16. Ahmad S, Bhagwati S, Kumar S, et al. Molecular modeling assisted identification and biological evaluation of potent cathepsin S inhibitors. J Mol Graph Model 2020;96:107512.
17. Chen G, Ni Y, Nagata N, et al. Lycopene Alleviates Obesity-Induced Inflammation and Insulin Resistance by Regulating M1/M2 Status of Macrophages. Mol Nutr Food Res 2019;63:e1900602.
18. Figueiredo JL, Aikawa M, Zheng C, et al. Selective cathepsin S inhibition attenuates atherosclerosis in apolipoprotein E-deficient mice with chronic renal disease. Am J Pathol 2015;185:1156-66.
19. Kitade H, Sawamoto K, Nagashimada M, et al. CCR5 plays a critical role in obesity-induced adipose tissue inflammation and insulin resistance by regulating both macrophage recruitment and M1/M2 status. Diabetes 2012;61:1680-90.
20. Ni Y, Nagashimada M, Zhan L, et al. Prevention and reversal of lipotoxicity-induced hepatic insulin resistance and steatohepatitis in mice by an antioxidant carotenoid, β-cryptoxanthin. Endocrinology 2015;156:987-99.

21. Livak KJ, Schmittgen TD. Analysis of relative gene expression data using real-time quantitative PCR and the 2(-Delta Delta C(T)) Method. Methods 2001;25:402-8.
22. Tong Y, Xu S, Huang L, et al. Obesity and insulin resistance: Pathophysiology and treatment. Drug Discov Today 2022;27:822-30.
23. Yao J, Wu D, Zhang C, et al. Macrophage IRX3 promotes diet-induced obesity and metabolic inflammation. Nat Immunol 2021;22:1268-79.
24. Turk V, Stoka V, Vasiljeva O, et al. Cysteine cathepsins: from structure, function and regulation to new frontiers. Biochim Biophys Acta 2012;1824:68-88.
25. Brown R, Nath S, Lora A, et al. Cathepsin S: investigating an old player in lung disease pathogenesis, comorbidities, and potential therapeutics. Respir Res 2020;21:111.
26. Yao X, Cheng F, Yu W, et al. Cathepsin S regulates renal fibrosis in mouse models of mild and severe hydronephrosis. Mol Med Rep 2019;20:141-50.
27. Kawato Y, Fukahori H, Nakamura K, et al. Potential benefit of the cathepsin S inhibitor, ASP1617, as a treatment for systemic lupus erythematosus. Eur J Pharmacol 2022;919:174826.
28. Rauner M, Föger-Samwald U, Kurz MF, et al. Cathepsin S controls adipocytic and osteoblastic differentiation, bone turnover, and bone microarchitecture. Bone 2014;64:281-7.
29. Yoo Y, Choi E, Kim Y, et al. Therapeutic potential of targeting cathepsin S in pulmonary fibrosis. Biomed Pharmacother 2022;145:112245.
30. Wei L, Shao N, Peng Y, et al. Inhibition of Cathepsin S Restores TGF-β-induced Epithelial-to-mesenchymal Transition and Tight Junction Turnover in Glioblastoma Cells. J Cancer 2021;12:1592-603.
31. Rosen ED, Spiegelman BM. Adipocytes as regulators of energy balance and glucose homeostasis. Nature 2006;444:847-53.
32. Dong H, Sun W, Shen Y, et al. Identification of a regulatory pathway inhibiting adipogenesis via RSPO2. Nat Metab 2022;4:90-105.
33. Muni Swamy G, Ramesh G, Devi Prasad R, et al. Astragalin, (3-O-glucoside of kaempferol), isolated from Moringa oleifera leaves modulates leptin, adiponectin secretion and inhibits adipogenesis in 3T3-L1 adipocytes. Arch Physiol Biochem 2022;128:938-44.
34. Li J, Gong L, Xu Q. Purinergic 2X7 receptor is involved in adipogenesis and lipid degradation. Exp Ther Med 2022;23:81.
35. Sun K, Kusminski CM, Scherer PE. Adipose tissue remodeling and obesity. J Clin Invest 2011;121:2094-101.
36. Buckner JH. Mechanisms of impaired regulation by CD4(+)CD25(+)FOXP3(+) regulatory T cells in human autoimmune diseases. Nat Rev Immunol 2010;10:849-59.
37. Sell H, Habich C, Eckel J. Adaptive immunity in obesity and insulin resistance. Nat Rev Endocrinol 2012;8:709-16.
38. Lumeng CN, Bodzin JL, Saltiel AR. Obesity induces a phenotypic switch in adipose tissue macrophage polarization. J Clin Invest 2007;117:175-84.
39. Kanda H, Tateya S, Tamori Y, et al. MCP-1 contributes to macrophage infiltration into adipose tissue, insulin resistance, and hepatic steatosis in obesity. J Clin Invest 2006;116:1494-505.
40. Hirahara L, Takase-Minegishi K, Kirino Y, et al. The Roles of Monocytes and Macrophages in Behçet's Disease With Focus on M1 and M2 Polarization. Front Immunol 2022;13:852297.
41. Xie L, Liu Y, Zhang N, et al. Electroacupuncture Improves M2 Microglia Polarization and Glia Anti-inflammation of Hippocampus in Alzheimer's Disease. Front Neurosci 2021;15:689629.
42. Canbay A, Bechmann L, Gerken G. Lipid metabolism in the liver. Z Gastroenterol 2007;45:35-41.
43. Zhai Z, Niu KM, Liu H, et al. Policosanol alleviates hepatic lipid accumulation by regulating bile acids metabolism in C57BL6/mice through AMPK-FXR-TGR5 cross-talk. J Food Sci 2021;86:5466-78.
44. Han H, Wang M, Zhong R, et al. Depletion of Gut Microbiota Inhibits Hepatic Lipid Accumulation in High-Fat Diet-Fed Mice. Int J Mol Sci 2022;23:9350.
45. Lee JH, Woo KJ, Kim MA, et al. Heat-Killed Enterococcus faecalis Prevents Adipogenesis and High Fat Diet-Induced Obesity by Inhibition of Lipid Accumulation through Inhibiting C/EBP-α and PPAR-γ in the Insulin Signaling Pathway. Nutrients 2022;14:1308.

(English Language Editor: L. Huleatt)

Cite this article as: Zheng J, Zhuang H, Zhang T, Wang Y, Ran T, He J, Han N, Duan J. Cathepsin S inhibitor reduces high-fat-induced adipogenesis, inflammatory infiltration, and hepatic lipid accumulation in obese mice. Ann Transl Med 2022;10(21):1172. doi: 10.21037/atm-22-5145

